High Meadows Environmental Institute

MECHANICAL & AEROSPACE ENGINEERING

# Progress in wind-forced breaking waves

**Nicolò Scapin**[1,2], Jiarong Wu[1,*], J. Thomas Farrar[3],
Bertrand Chapron[4], Stéphane Popinet[5] and Luc Deike[1,2]

**Basilisk (Gerris) Users' Meeting 2025 (BGUM)**
**Oxford University, UK (July 7th - 9th, 2025)**

1. Department of Mechanical and Aerospace Engineering (MAE), Princeton University, US
2. High Meadows Environmental Institute (HMEI), Princeton University, US
3. Woods Hole Oceanographic Institution (WHOI), US
4. IFREMER, Univ. Brest, CNRS, IRD, Laboratoire d'Océanographie Physique et Spatiale (LOPS), France
5. CNRS, Institut Jean Le Rond d'Alembert - Sorbonne Université, France

* Current affiliation: Courant Institute of Mathematical Sciences, New York University, US

# Wind-forced breaking waves

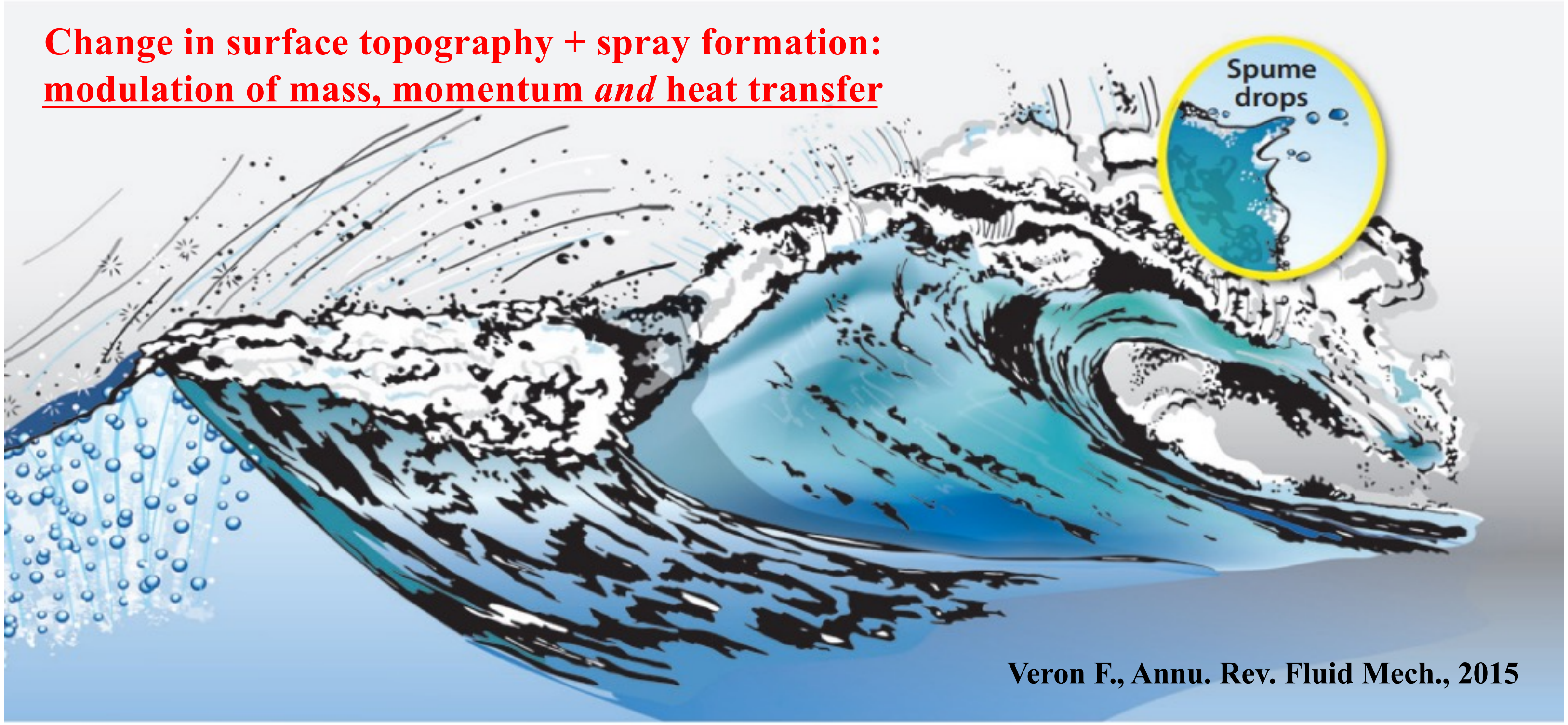


**Waves** and **wave breaking** modulate the exchanges
of **momentum**, **energy** and **mass** at the ocean-atmosphere interface

# Wind-forced breaking waves

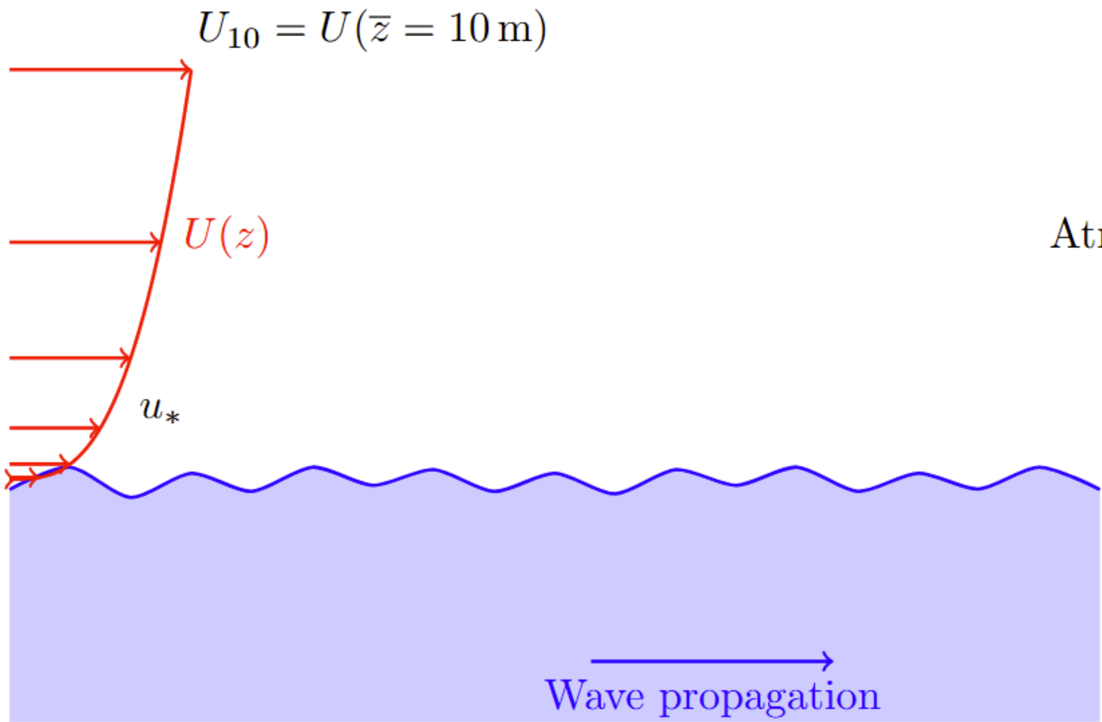


Atmosphere → **Turbulent airflow**

**Momentum/energy fluxes**

**Waves/ underwater currents**

← Ocean

**Dissipation due to viscous effects and wave breaking**

# Wind-wave interaction problem: physical parameters

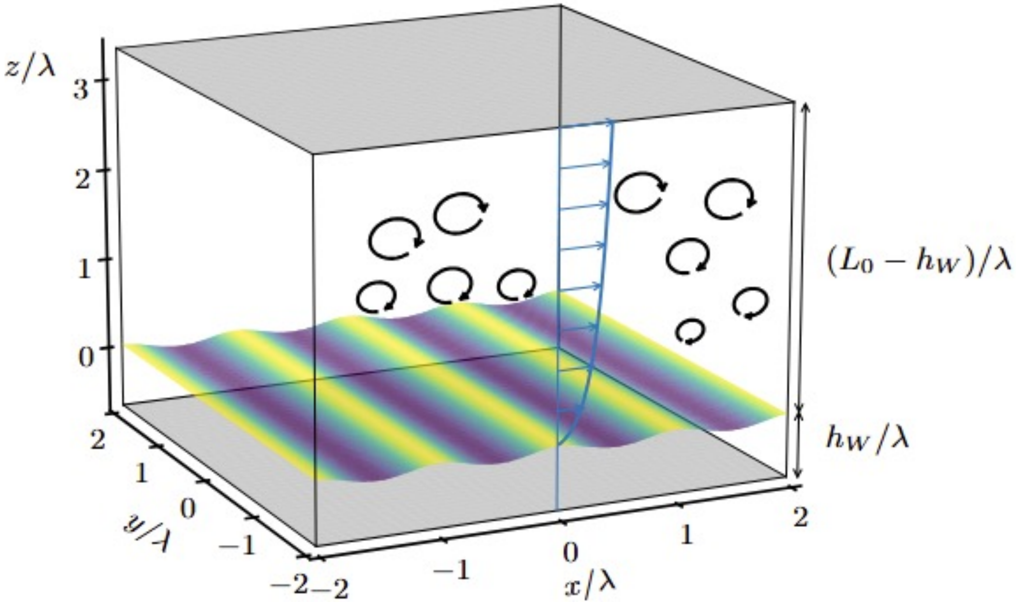


**Fully-resolved direct numerical simulations** using VoF (`src/vof.h`) to capture the **wave field** and the two-phase modules to solve the **flow field** (`navier-stokes/centered.h` and `navier-stokes/conserving.h`)

**11 physical parameters with 3 units ([M], [L], [T])**

$$\rho_a, \rho_w, \mu_a, \mu_w, (L_0 - h_W), h_W, \lambda, a_0, \sigma, |g|, u_*$$

$\downarrow$ ***Π* theorem**

**8 physical dimensionless parameters**

- **Density ratio:** $\rho_a/\rho_w$
- **Ratios of length scales:** $(L_0 - h_W)/\lambda$, $h_W/\lambda$

- **Friction Reynolds number:** $Re_{*,\lambda} = \frac{\rho_a u_* \lambda}{\mu_a}$
- **Wave Reynolds number:** $Re_{wave} = \frac{\rho_w c \lambda}{\mu_w}$
- **Bond number:** $Bo = \frac{|\boldsymbol{g}|(\rho_w - \rho_a)\lambda^2}{4\pi^2\sigma}$
- **Initial wave steepness:** $a_0 k$
- **Friction velocity over wave speed:** $\frac{u_*}{c}$

# Configuration set-up

- **Initial condition in Air**: fully-developed turbulence (generated with a precursor simulation)
- **Initial condition in Water**: potential flow solution of a third-order Stokes wave.

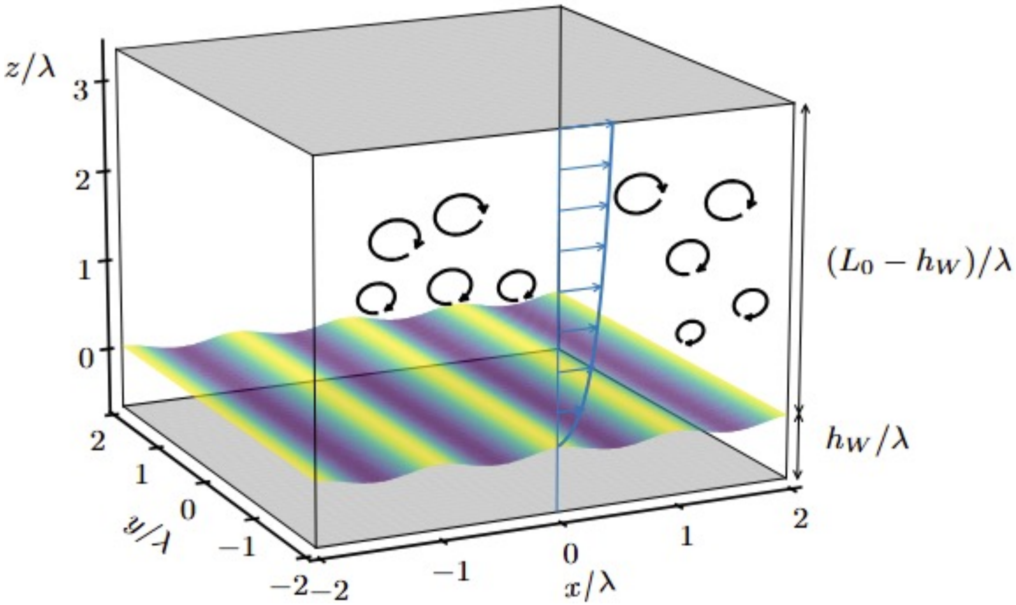


**Computational domain:**
- $4\lambda \times 4\lambda \times 4\lambda$, $h_w \approx 0.64\lambda, L_0 - h_w \approx 3.36\lambda$
- x-y: periodic directions; z: free-slip conditions;
- Grid resolution: $L^{10} - L^{11}$(i.e. $1024^3 - 2048^3$);

**We fix**:

$Re_* = 720, Re_w = 2.5 \cdot 10^4, Bo = 200, a_0 k = 0.3$

**We vary** (in the **high-wind speed** regime):

$$\frac{u_*}{c} = 0.3 - 0.4 - 0.5 - 0.7 - 0.9;$$

# Part 1: Exchanged momentum fluxes (1/2)

## Dimensionless momentum flux, $C_D$

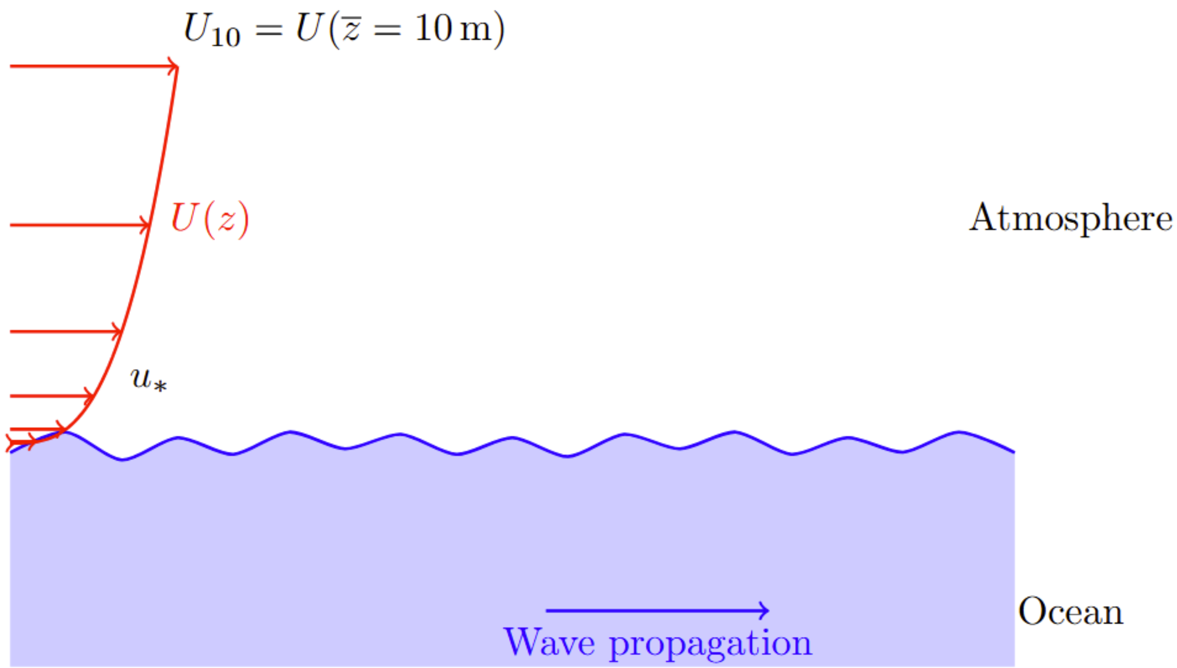


$$C_D = \frac{u_*^2}{U^2(\bar{z} = 10\ m)}$$

**Drag coefficient:**
the imposed stress (per unit of air density) over $\boldsymbol{U_{10}^2}$

$$\boldsymbol{U_{10} = \frac{u_*}{\kappa} \log\left(\frac{\bar{z}}{z_0}\right)}$$

$$C_D = \frac{\kappa^2}{\log^2\left(\frac{\bar{Z}}{z_0}\right)}$$

**Drag coefficient** function of the **surface roughness:** $z_0$

# Part 1: Exchanged momentum fluxes (2/2)

## Dimensionless momentum flux, $C_D$

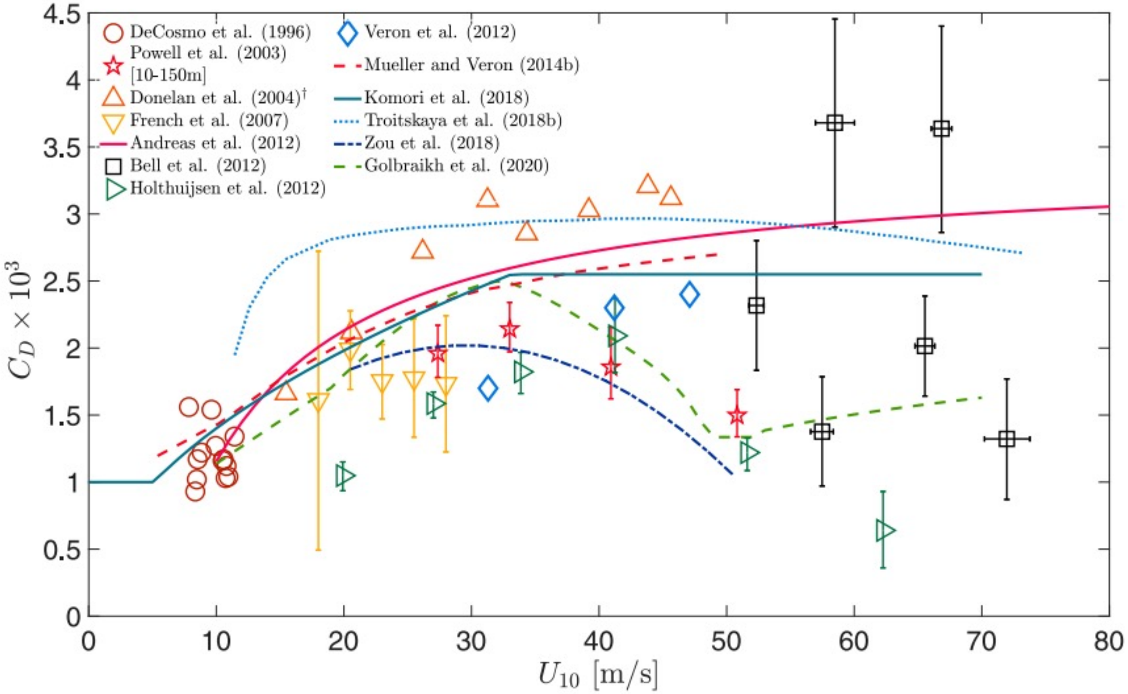


Sroka & Emmanuel (JPO, 2021)

--> $\boldsymbol{C_D}$ initially increases with $\mathbf{U_{10}}$, but at higher wind speed, it develops a saturation.

--> **Large uncertainty** and **data scattering** as $U_{10}$ increases.

***Questions:***

(a) What's the **physical mechanism(s)** behind the non-linear variation of $C_D$ with $U_{10}$?

(b) What's the role of **wave breaking**?

**u*/c = 0.9**

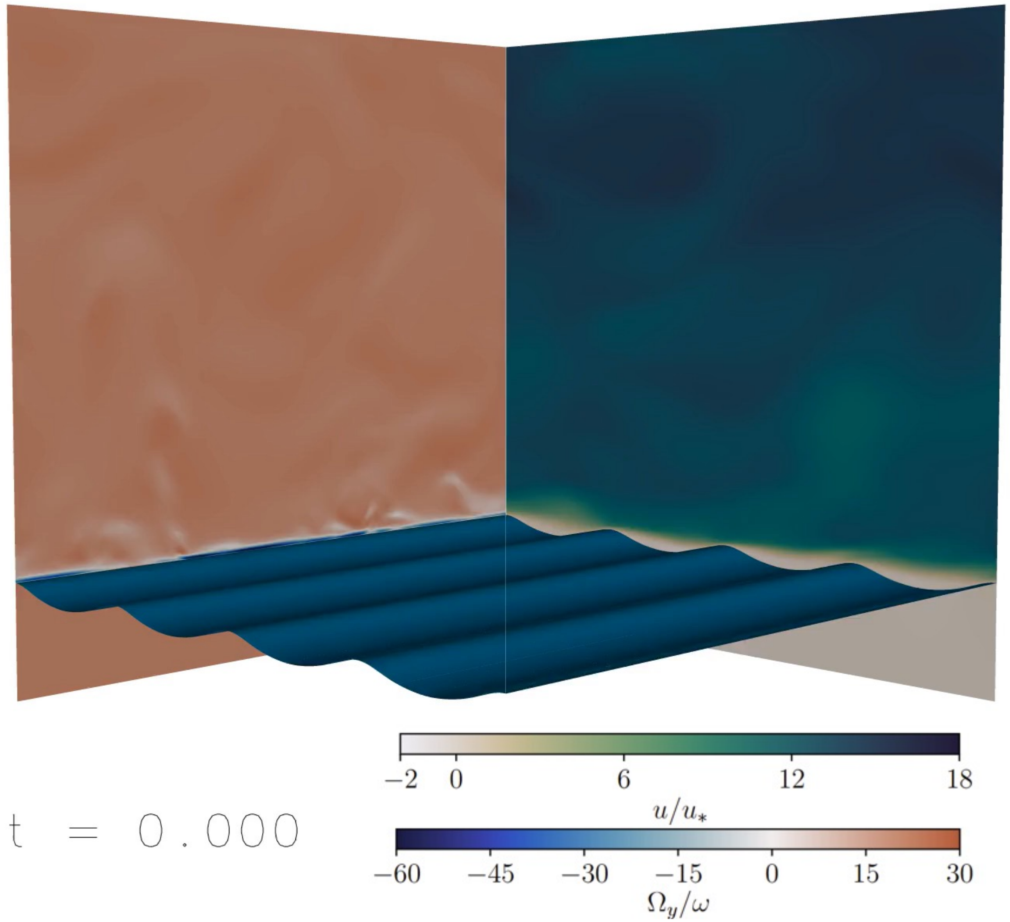


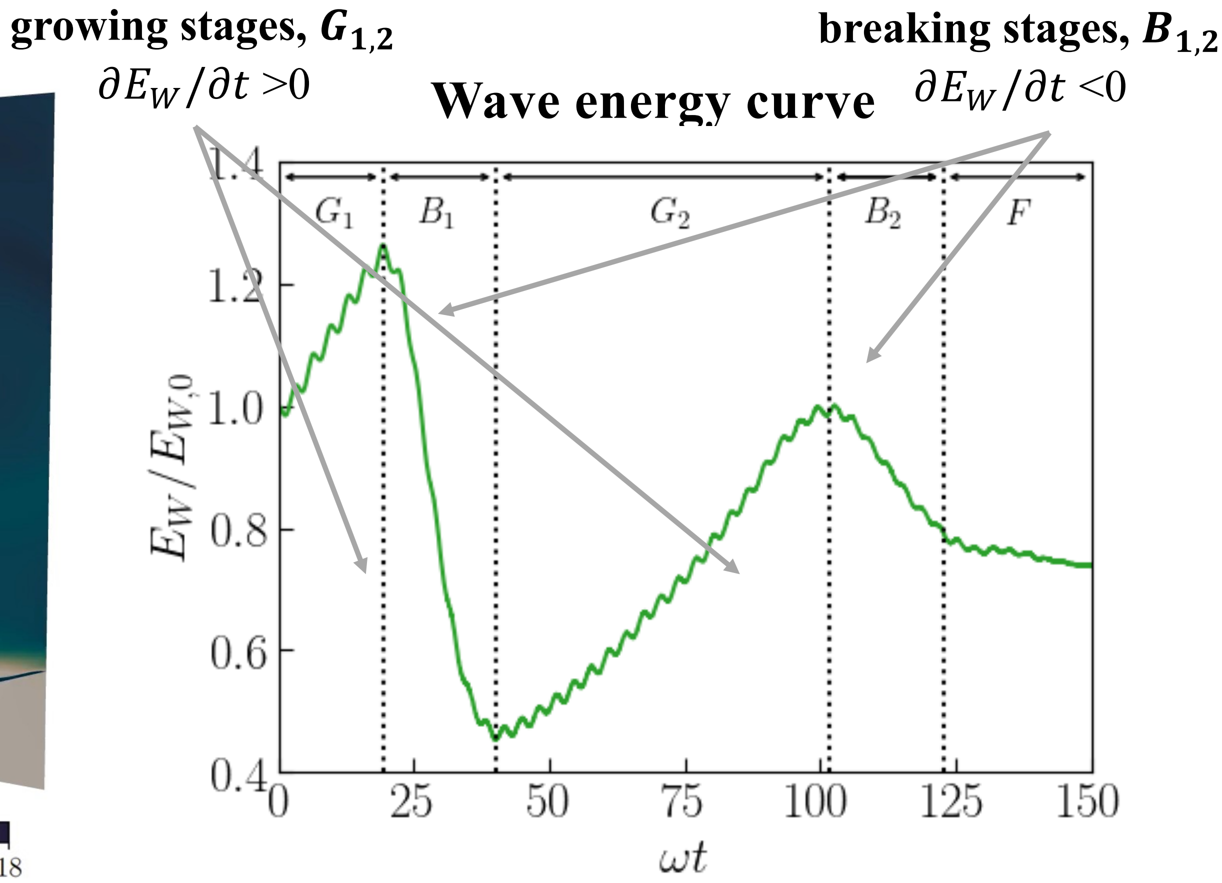


$$E_w(t) = \rho_w |\boldsymbol{g}| \int_{\Omega_w} (z - z_0) dV$$

**<u>The instantaneous change in $E_W(t)$, i.e. change in a(t)k</u>**

(1) Affects the exchanged **momentum**, i.e. ***pressure and viscous forces***, between air and water;

(2) Modulates the **airflow**;

# Momentum fluxes/exchanged forces

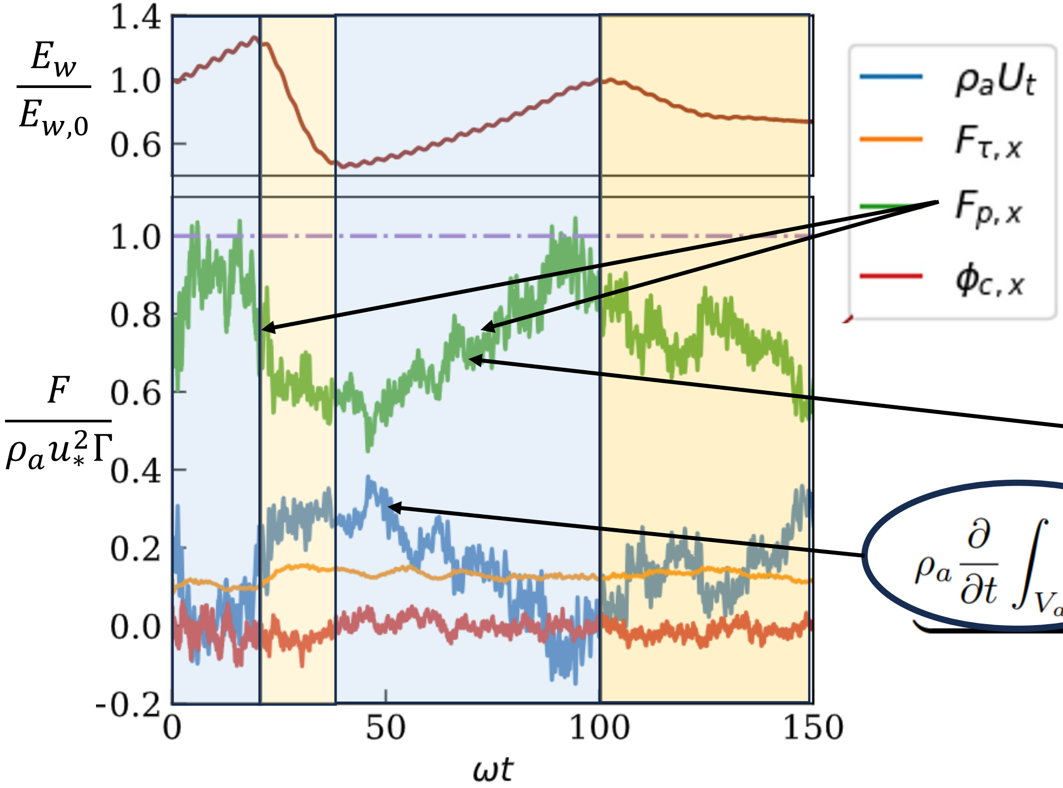


**Growing stage:** increase in the pressure force

**Breaking stage:** drop in the pressure force

***Streamwise momentum budget in the air***

$$\underbrace{\rho_a \frac{\partial}{\partial t}\int_{V_a} u dV - \rho_a u_*^2 \frac{V_a}{4\lambda - h_w}}_{\rho_a U_t} + \underbrace{\rho_a \int_{\Gamma} \nabla \cdot (u\mathbf{u}_{ri}) dS}_{\phi_{c,x}} = F_{p,x} + F_{\tau,x}$$

the **compensation for pressure force** comes from the change in the **mean flow** and partially from the **viscous contribution** → **Airflow modulation**

# Airflow modulation

Streamwise velocity profile (in a ***wave-following coordinate***) during the **pre-breaking $G_1$, breaking** and **post-breaking stages $G_{2,a}$**

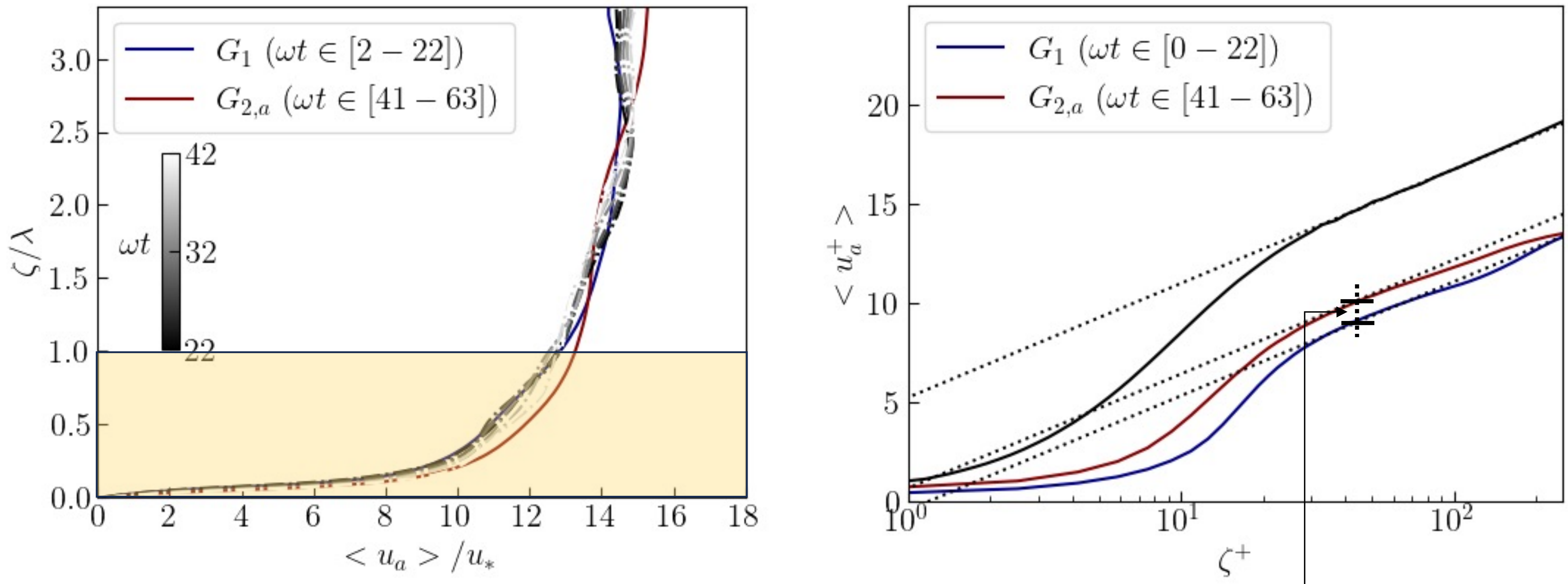


During wave-breaking the flow progressively accelerates in the region near the wave field, $\boldsymbol{\zeta < \lambda}$ → Drag reduction

# Aerodynamic drag coefficient, $C_{D,a}$, over breaking waves

During the breaking: *(1)* **reduction of the pressure force**, *(2)* **flow acceleration in the region close to the wave field**

$$C_{D,a} = \frac{2\bar{F}_p}{\rho_a \Gamma \bar{U}^2 \ (z = \frac{\lambda}{2})}$$

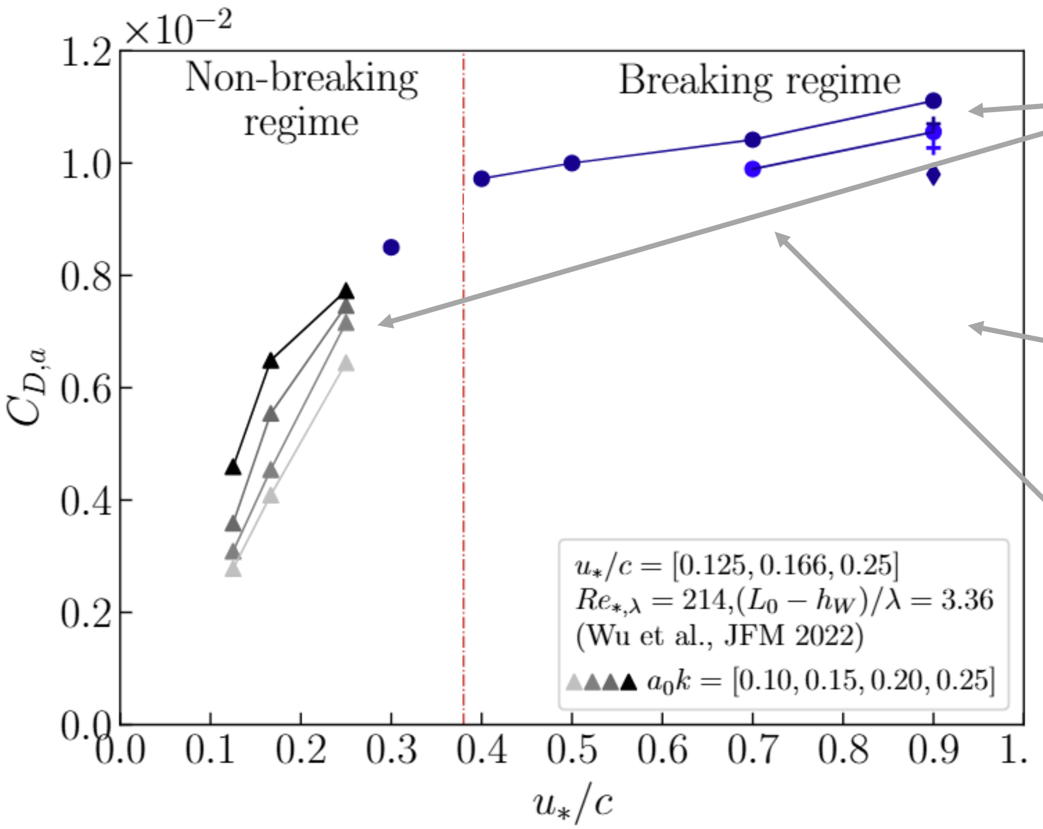


**<u>Growing stages</u>:** $C_{D,a}$ continuously increases (larger pressure force with $u_*/c$)

**<u>Breaking stages</u>:** during the growing stage, $C_{D,a}$ continuously increases with. During the breaking stage, $C_{D,a}$ decreases with $u_*/c$

**<u>Mean Saturation</u>** of $C_{D,a}$ is observed when wave breaking **is accounted for**.

# Drag coefficient over breaking waves

Using the classical definition of the **drag coefficient in physical oceanography**

$$C_D = \frac{u_*^2}{U_{10}^2} \xrightarrow{U_{10}=\frac{u_*}{\kappa}\log\left(\frac{z}{z_0}\right)} C_{D,10} = \frac{\kappa^2}{\log^2\left(\frac{z\,=\,10\,m}{z_0}\right)}$$

**Extracted from the velocity profile**

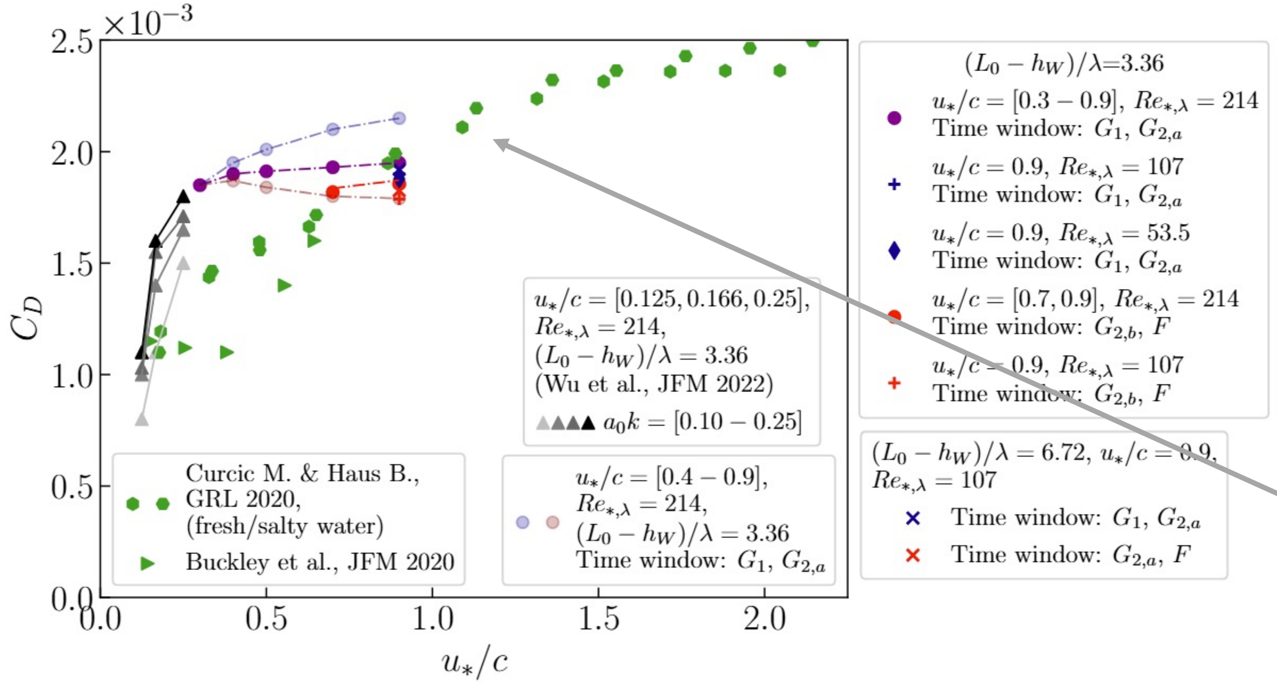


- Qualitatively similar trend to the aerodynamic drag coefficient $C_{D,A}$;
- **Drag saturation** and **reduction** occurs when the **wave breaking dynamics** is included.
- Remarkable agreement with laboratory experiments at similar $u_*/c$.
- **Small deviations** attributed to *(a)* multiscale nature of the wave field in the lab, *(b)* several hundreds of breaking cycles

# Part 2: Wave breaking-induced dissipation

when wave break: **energy is dissipated and transfer into the water column**

**Large scatter of field data for the dissipation** **Enhanced turbulence dissipation**

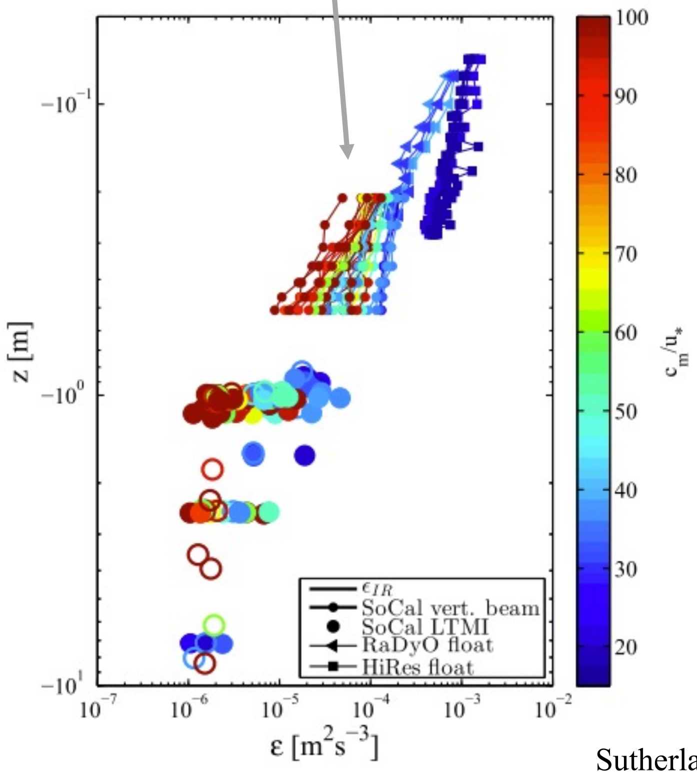


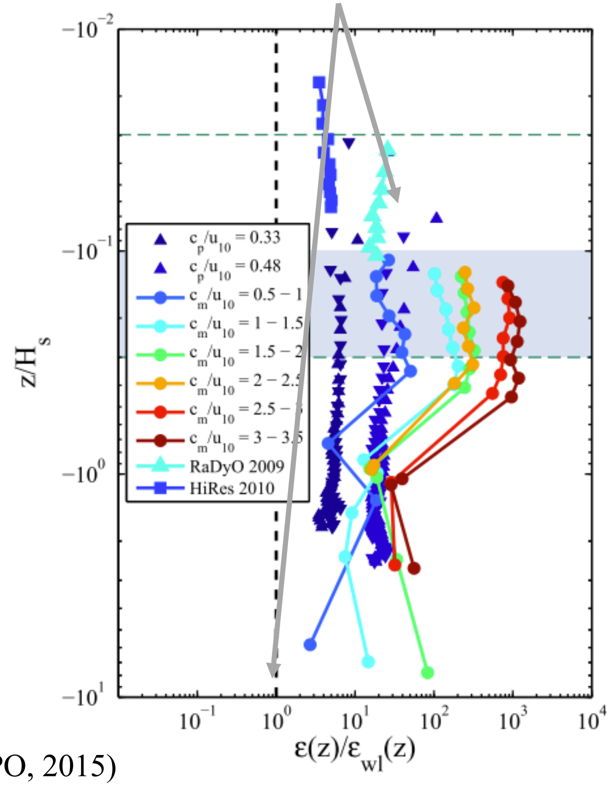


Sutherland & Melville (JPO, 2015)

**How wave breaking modulate the underwater dissipation?**

# Wave breaking-induced dissipation (1/2)

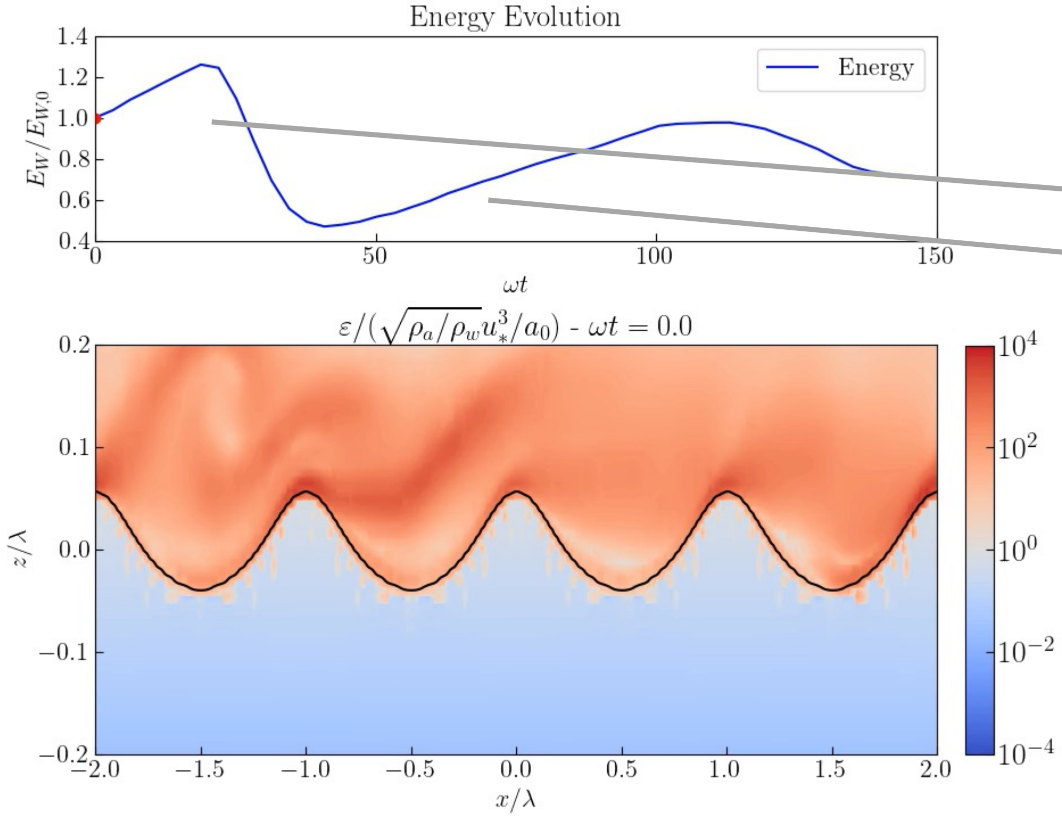


**Profile during $G_1$, $B_1$ and $G_2$**

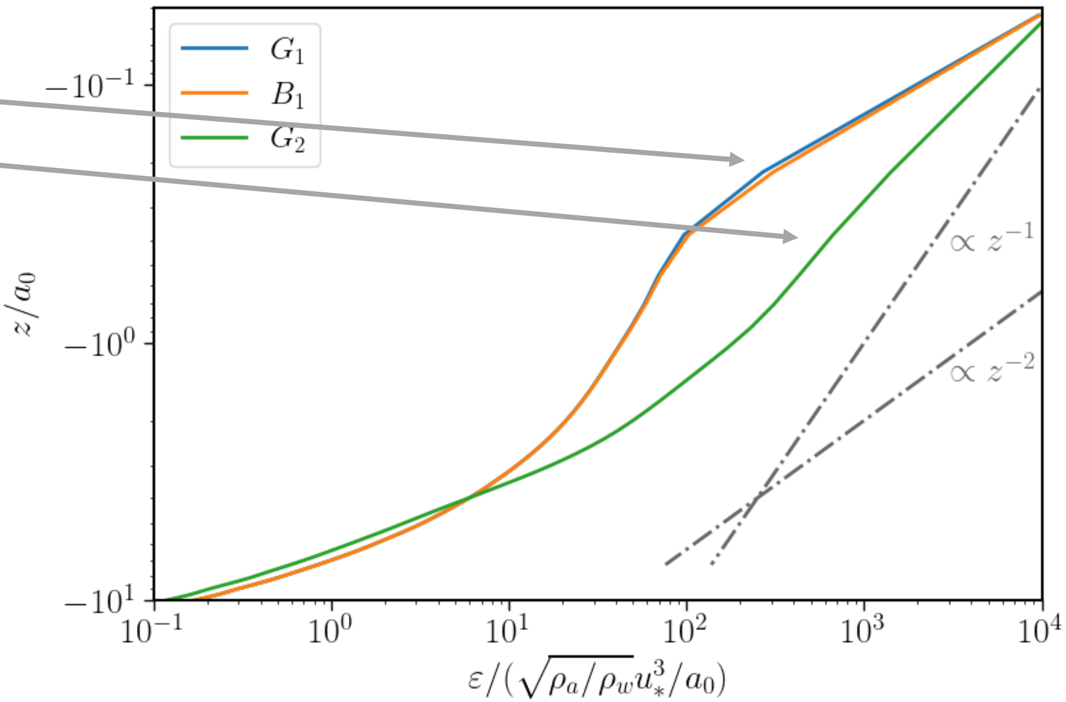


Dissipation negligible during $G_1$

Dissipation starts to become larger during $B_1$ and is transported in the water column during $B_2$

**Wave breaking promotes the transition of the dissipation profile!**

# Scaling the underwater energy dissipation (1/3)

Sutherland and Melville (JPO, 2015) proposed to rescale $\varepsilon$ as

$$\frac{\rho_w \varepsilon H_s}{S_{in}} = f\left(\frac{z}{H_s}\right)^{-1} \qquad S_{in} = F_{p,x} c \approx \rho_a u_*^2 c$$

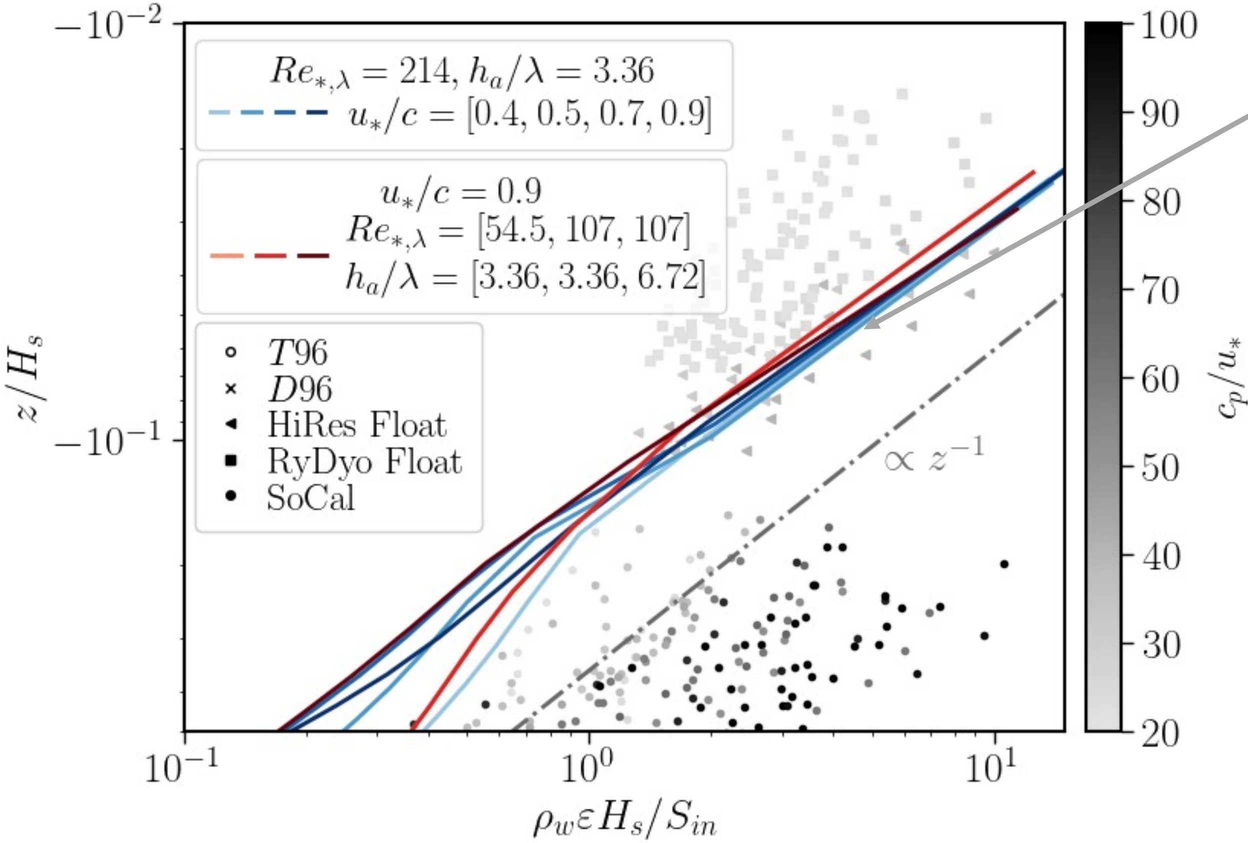


- **A very good collapse** of the dissipation profiles within $0.1H_s$
- **Numerical results are compatible with the field data** at the lowest wave age near the surface

# Scaling the underwater energy dissipation (2/3)

The validity of the scaling proposed in Sutherland and Melville (JPO, 2015) lead to two observations:

***The wall-layer scaling argument is an incorrect scaling for the turbulent dissipation***

**Wall-layer scaling** $\varepsilon_{wl} = \frac{u_*^3(\rho_a/\rho_w)^{0.5}}{\kappa}\frac{u_*^3}{z}$

**Present scaling** $\frac{\rho_w \varepsilon(z) H_s}{S_{in}} = A\frac{H_s}{z} \rightarrow \varepsilon(z) = A\frac{\rho_a}{\rho_w}\frac{u_*^2 c}{z}$

***Balanced between wind input and energy dissipation***

$$\frac{\rho_w \varepsilon(z) H_s}{S_{in}} = A\frac{H_s}{z} \longrightarrow \underbrace{\int_{-h_0}^{\eta} \varepsilon(z)dz}_{S_{ds}} \sim S_{in}$$

$$\boldsymbol{S_{in} \sim S_{ds}}$$

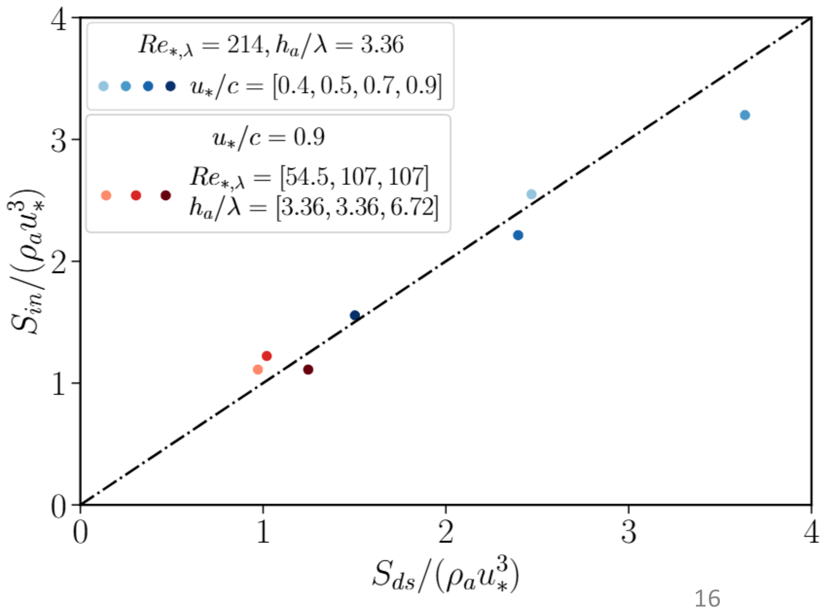

# Scaling the underwater energy dissipation (3/3)

$$S_{in} \sim S_{ds} = \frac{\rho_w}{g}\int b\Lambda(c)c^5 dc = \frac{\rho_w}{g}\frac{bc^5}{L_c}$$

Philips (JFM 1985)

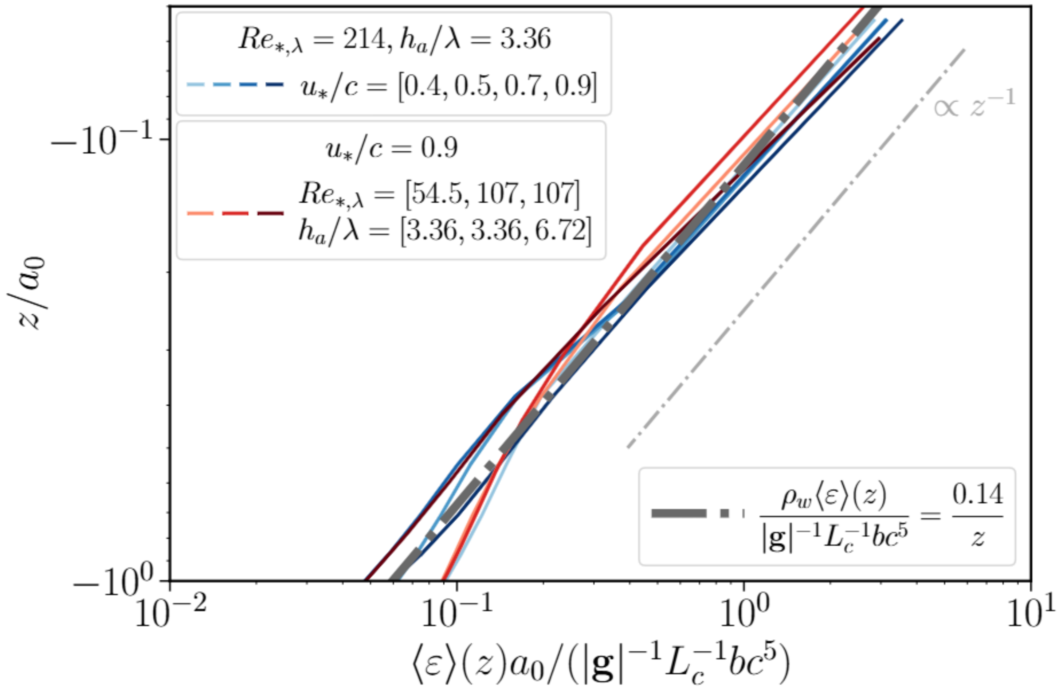


- **A very good collapse** of the dissipation profiles within $0.1H_s$
- **Given** $S_{in} \sim S_{ds}$, this **dissipation-based scaling** is fully consistent with the **wind-input based scaling**.

**Consistent with our understanding of wave breaking:**

wave breaking occurs when fluid inertia overcome restoring forces. The cause, e.g. wind, sets the onset of breaking. Once breaking starts, the energy loss is independent from the cause

# Conclusions

***Momentum fluxes***

- **Direct numerical simulations** of wind-forced wave breaking at high wind speed
- Analysis performed **by separating the growing** and **the breaking cycle**
- **Nonmonotonous behaviour** of the pressure force which reduces after the breaking stage (even without droplets). **Reduction is linked to the airflow modulation**
- **Saturation of $C_{D,a}$ and $C_D$** controlled by wave breaking dynamics

***Breaking-induced dissipation***

- **Wave breaking is sufficient to promote the transition of $\varepsilon$** to $\sim z^{-1}$
- **New scaling law** to unify the dissipation profile across different $u_*/c$

N. Scapin et al., "*Momentum fluxes in wind-forced breaking waves*", Journal of Fluid Mechanics
N. Scapin et al., "*Growth and dissipation in wind-forced breaking waves*", submitted to Geophysical Research Letters

**Simulations files are not in the sandbox yet, but they will be added soon!**

High Meadows Environmental Institute

MECHANICAL & AEROSPACE ENGINEERING

# Numerical methodology

Direct solution of *(1)* continuity equation (incompressibility constraint) with *(2)* the momentum equation for a **two-phase system**

$$\nabla \cdot \boldsymbol{u} = 0$$

$$\rho\left(\partial_t \boldsymbol{u} + \nabla \cdot (\boldsymbol{u}\boldsymbol{u})\right) = -\nabla p + \nabla \cdot \left(\mu(\nabla \boldsymbol{u} + \nabla \boldsymbol{u}^T)\right) + \sigma\kappa\delta_\Gamma + \rho\boldsymbol{g}$$

**<u>Main features of the numerical algorithm:</u>**

- **Sharp-interface formulation** for the interface advection (geometric VoF)
- **Momentum consistent formulation** to ensure robustness at high density ratio
- **Well-balanced formulation** to avoid artificial parasitic currents at the interface
- **Adaptive mesh-refinement (AMR)** techniques based on wavelet transformation